

# Semiactive Control Methodologies for Suspension Control with Magnetorheological Dampers

Mauricio Zapateiro, Francesc Pozo, Hamid Reza Karimi and Ningsu Luo

**Abstract**—Suspension systems are one of the most critical components of transportation vehicles. They are designed to provide comfort to the passengers, to protect the chassis and the freight. Suspension systems are normally provided with dampers that mitigate these harmful and uncomfortable vibrations. In this paper, we explore two control methodologies (in time and frequency domain) used to design semiactive controllers for suspension systems that make use of magnetorheological dampers. These dampers are known because of their nonlinear dynamics which requires the use of nonlinear control methodologies for an appropriate performance. The first methodology is based on the backstepping technique which is applied with adaptation terms and  $H_\infty$  constraints. The other methodology to be studied is the Quantitative Feedback Theory (QFT). Despite QFT is intended for linear systems, it can still be applied to nonlinear systems. This can be achieved by representing the nonlinear dynamics as a linear system with uncertainties that approximately represents the true behavior of the plant to be controlled. The semiactive controllers are simulated in MATLAB/Simulink for performance evaluation.

**Index Terms**—Semiactive control; backstepping; Quantitative Feedback Control; Suspension control; magnetorheological damper.



## 1 INTRODUCTION

Suspension systems are one of the most critical components of a vehicle. They are designed to provide comfort to the passengers, to protect the chassis and the freight. In the case of aircrafts, the landing gears fulfill these tasks. Not only are they designed to provide comfort during taxiing but absorb the energy during touch down. Suspension systems are normally provided with dampers that mitigate these harmful and uncomfortable vibrations [1]. In general, these dampers are passive, meaning that they are tuned once during design and construction not allowing for further changes once they are installed. This class of dampers is still in wide usage, but the fact that passive dampers cannot change their dynamics in response to different inputs is a drawback because they may not respond as expected in every single circumstance. This is why active and semiactively tuned dampers are being widely studied. As a result, several active and semiactive damping devices are already installed in commercially distributed vehicles and big efforts towards the implementation of active and semiactive dampers in aircraft are being done [2]. Compared with passive dampers, active and semiactive

devices can be tuned due to their flexible structure. One of the drawbacks of active dampers is that they may become unstable if the controller fails. On the contrary, semiactive devices are generally stable and thus, they act as pure passive dampers in case of control failure [3]. Among different semiactive devices, magnetorheological (MR) fluid dampers are the one of the most attractive and useful ones. MR dampers can generate high yield strength, have low costs of production, require low power, and have fast response and small size. However, they are characterized by a nonlinear dynamics (typically hysteresis) which makes mathematical treatment challenging, especially in the modeling and identification of the hysteretic dynamics and the development of control laws for its implementation through MR dampers for vibration mitigation purposes [4].

This increasing interest in the control of active and semiactive suspension systems has led to a number of control methodologies. For instance, in [5], it is proposed a semiactive controller based on a hybrid approach that combines a nonlinear PID term based on the expression of the shock absorber viscous force contribution; in [3], a kind of Nonlinear Model Predictive Control algorithm (NMPC) for semiactive landing gears is developed using Genetic Algorithms (GA) as the optimization technique and chooses damping performance of landing gear at touch down to be the optimization object; in [6] a fuzzy adaptive output feedback controller to control landing gear shimmy through active damping is proposed; a sky-hook semiactive control strategy was studied by Yao *et al.* [7] and also by Sankaranarayanan *et al.* [8]. The system was equipped with an MR damper and it was shown to be superior to other passive and active control strategies.

- M. Zapateiro and F. Pozo are with CoDALab ([codalab.ma3.upc.edu](mailto:codalab.ma3.upc.edu)), Department of Applied Mathematics III, Escola Universitària d'Enginyeria Tècnica Industrial de Barcelona, Universitat Politècnica de Catalunya - BarcelonaTECH, 08036 Barcelona, Spain.  
E-mails: [mauricio.zapateiro@upc.edu](mailto:mauricio.zapateiro@upc.edu), [francesc.pozo@upc.edu](mailto:francesc.pozo@upc.edu)
- H.R. Karimi is with the Department of Engineering, Faculty of Technology and Science, UNiversity of Agder, N-4898 Grimstad, Norway.  
E-mail: [hamid.r.karimi@uia.no](mailto:hamid.r.karimi@uia.no)
- N. Luo is with the Institute of Informatics and Applications, University of Girona, 17071 Girona, Spain.  
E-mail: [ningsu.luo@udg.edu](mailto:ningsu.luo@udg.edu)

A neural network control was designed by Guo et al. [9] for a quarter car model with a magnetorheological damper for vibration reduction. This neural network consists of only one hidden layer making it very fast. As a result, the controller was able to achieve acceleration reductions of up to 55%. Optimal control with preview was studied by Karlsson et al. [10]. In their work, the car acceleration was reduced and as a consequence, ride control and passenger comfort were improved. Moreover, the preview contributed to reduce the RMS tyre deflection and hence, vehicle landing performance was also improved.

$H_\infty$  control techniques have also been extensively studied. Du et al. [11] explored a non-fragile  $H_\infty$  control for an active vehicle suspension system. The output feedback controller was designed using linear matrix inequalities (LMI) and GA. Their objective was to minimize the mass acceleration, suspension deflection and tyre deflection and the effectiveness of the controllers was validated through numerical simulations on a quarter-car model. These authors [12] have also explored the semiactive suspension case, this time using an MR damper. A static output feedback  $H_\infty$  controller was designed using suspension deflection and mass velocity as feedback signals. The work was validated through simulations of a quarter-car model. Gao et al. [13] proposed a load-dependent controller for an active vehicle suspension system. The multi-objective controller was designed using LMI's following an approach based on a parameter-dependent Lyapunov function. The results were validated, as in the previous cases, through simulations of a quarter-car model. Gao et al. [14] studied the effects of data sampling in an active suspension system. To this end, they used an input delay approach in such a way to obtain that the system with sampled measurements was transformed into a continuous-time system with a delay in the state. An  $H_\infty$  controller was developed using LMI's. Gao et al. [15] went a step further by considering the problem of the passenger comfort. In this work, they considered the problem of the seat suspension. The controller design is cast into a convex multi-objective optimization problem with LMI constraints.

Backstepping is a recursive design for systems with nonlinearities not constrained by linear bounds. The ease with which backstepping incorporated uncertainties and unknown parameters contributed to its instant popularity and rapid acceptance. Applications of this technique have been recently reported ranging from robotics to industry or aerospace [16], [17], [18]. Backstepping control has also been explored in some works about suspension systems. For example, Zapateiro et al. [19] designed a semiactive backstepping control combined with Neural Network techniques for a system with MR damper. On the other hand, Nguyen et al. [20] studied a hybrid control of active suspension systems for quarter-car models with two-degree-of-freedom. It was implemented by controlling the linear part with  $H_\infty$  techniques and the

nonlinear part with an adaptive controller based on backstepping. Quantitative Feedback Theory (QFT) has also been explored in a few works. For example, one of the first works involving QFT in active suspension systems is that by Liberzon et al. [21]. The controller was designed to improve cross-country mobility without the need of state estimation. The model of the system plant was linearized with respect to its harmonic responses, yielding generalized describing functions in the form of amplitude and frequency-dependent function values that define the plant templates. In [22], Amani et al. compared the performance of  $H_\infty$  and a QFT controllers. The results showed that the body acceleration was lower in the QFT-controlled case than in its  $H_\infty$  counterpart. In general, the QFT performance was better or at least comparable to that of the  $H_\infty$  controller. A QFT controller was also proposed by Taha et al. [23] to reduce the chattering of the main sliding mode controller. The QFT controller was designed inside the boundary layer to reduce the oscillations around the sliding surface.

Previous works -theoretical and practical- on Backstepping and QFT (see the references above) have shown the feasibility of practical implementation in vibrating systems thanks to the low numerical complexity that these control laws imply and their overall good performance when accounting for different design constraints at the same time. Due to the promising features of these control techniques in different applications, in this paper, as an extension to previous works, we propose two different semiactive control laws based on Backstepping and QFT for suspension systems equipped with MR dampers. An adaptive backstepping control with  $H_\infty$  techniques is presented. To the best of the authors' knowledge, this idea has not been deeply developed, being the work by Li and Liu [24] one example on this topic. Their method integrates the adaptive dynamics surface control and  $H_\infty$  control techniques guaranteeing that the output tracking error satisfies the  $H_\infty$  tracking performance [25]. Thus, our contribution regarding this issue is two-fold: first, this paper extends previous works on backstepping problem; second, by utilizing an adaptive technique, using a Lyapunov function and a suitable change of backstepping variables, we derive the explicit expression of the controllers to satisfy both asymptotic stability and an  $H_\infty$  performance for the controlled system. On the other hand, we also develop in this paper a semiactive controller based on QFT. In order to apply the QFT, some linearization must be performed. The interest in QFT lies in the fact that it allows for including in the design process several constraints related to uncertainties, unknown disturbances, actuator limitations and robustness. We use the approach presented in previous works [26], [27] in which the damper is represented as a linear system with uncertain parameters that approximately represents its dynamics. Then the QFT design process is followed as if it were an uncertain linear system. The design process accounts for robustness, disturbance rejection and control effort

issues.

The paper is organized as follows. Section 2 presents the mathematical details of the system to be controlled. In Section 3, the backstepping controller is developed. In Section 4, the QFT control formulation details are outlined. Section 5 shows the numerical results and in Section 6 the conclusions are drawn.

## 2 SUSPENSION SYSTEM MODEL

The suspension system can be modeled as a quarter car model, as shown in Figure 1. It is composed of two subsystems: the tyre subsystem and the suspension subsystem. The tyre subsystem is represented by the wheel mass  $m_u$  while the suspension subsystem consists of a sprung mass,  $m_s$ , that resembles the vehicle mass. The compressibility of wheel pneumatic is  $k_t$ , while  $c_s$  and  $k_s$  are the damping and stiffness of the uncontrolled suspension system. The following state variables are used to model the system:

- $x_1$  is the tyre deflection
- $x_2$  is the unsprung mass velocity
- $x_3$  is the suspension deflection
- $x_4$  is the sprung mass velocity.

Thus, the state space representation of the system of Figure 1 is given by [28]:

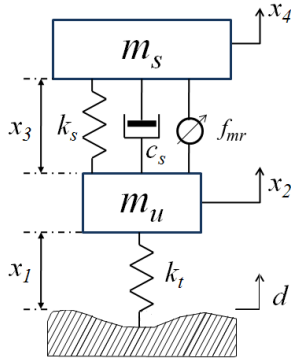


Fig. 1. Quarter car suspension model

- Tyre subsystem:

$$\begin{aligned} \dot{x}_1 &= x_2 - d \\ \dot{x}_2 &= -\frac{k_t}{m_u}x_1 + \rho u \end{aligned} \quad (1)$$

- Suspension subsystem:

$$\begin{aligned} \dot{x}_3 &= -x_2 + x_4 \\ \dot{x}_4 &= -u \end{aligned} \quad (2)$$

where  $\rho = m_s/m_u$ ,  $d$  is the velocity of the input disturbance and  $u$  is the acceleration input due to the damping subsystem. The input  $u$  is given by:

$$u = \frac{1}{m_s}(k_s x_3 + c_s(x_4 - x_2) - f_{mr}) \quad (3)$$

where  $f_{mr}$  is the damping force generated by the semi-active device.

In order to formulate the backstepping controller, the state space model of Equations (1) - (2) must be first written in strict feedback form [29]. Therefore, the following coordinate transformation is performed [28]:

$$\begin{aligned} z_1 &= x_1 + \frac{\rho}{\rho+1}x_3 \\ z_2 &= \frac{1}{\rho+1}x_2 + \frac{\rho}{\rho+1}x_4 \\ z_3 &= x_3 \\ z_4 &= -x_2 + x_4 \end{aligned} \quad (4)$$

The system, represented in the new coordinates, is given by:

- Tyre subsystem:

$$\begin{aligned} \dot{z}_1 &= z_2 - d \\ \dot{z}_2 &= -k_t[m_u(\rho+1)]^{-1}z_1 + \rho k_t[m_u(\rho+1)^2]^{-1}z_3 \end{aligned} \quad (5)$$

- Suspension subsystem:

$$\begin{aligned} \dot{z}_3 &= z_4 \\ \dot{z}_4 &= k_t m_u^{-1}z_1 - k_t \rho [m_u(\rho+1)]^{-1}z_3 - (\rho+1)u \end{aligned} \quad (6)$$

Substitution of the expression for  $u$  (Equation (3)) into Equation (6) yields:

$$\begin{aligned} \dot{z}_3 &= z_4 \\ \dot{z}_4 &= k_t m_u^{-1}z_1 - k_t \rho [m_u(\rho+1)]^{-1}z_3 - \\ & \quad (\rho+1)m_s^{-1}[k_s x_3 + c_s(x_4 - x_2) - f_{mr}] \\ &= -[k_t m_s \rho (\rho+1)^{-1} + (\rho+1)k_s m_u](m_u m_s)^{-1}z_3 + \\ & \quad k_t m_u^{-1}z_1 - (\rho+1)m_s^{-1}c_s z_4 + (\rho+1)m_s^{-1}f_{mr} \\ &= d_i - a_k z_3 - a_c z_4 + a_f f_{mr} \end{aligned} \quad (7)$$

where  $a_k = [k_t m_s \rho (\rho+1)^{-1} + (\rho+1)k_s m_u](m_u m_s)^{-1}$ ,  $a_c = (\rho+1)m_s^{-1}c_s$  and  $a_f = (\rho+1)m_s^{-1}$ ;  $d_i = k_t m_u^{-1}z_1$  reflects the fact that the disturbance enters to the suspension subsystem through the tyre subsystem.

The MR damper that the suspension system is equipped with is modeled according to the following Bouc-Wen model [30]:

$$f_{mr} = c_0(v)z_4 + k_0(v)z_3 + \alpha(v)\zeta \quad (8)$$

$$\dot{\zeta} = -\delta|z_4|\zeta|\zeta|^{n-1} - \beta z_4|\zeta|^n + \kappa z_4 \quad (9)$$

where  $\zeta$  is an evolutionary variable that describes the hysteretic behavior of the damper,  $z_4$  is the piston velocity,  $z_3$  is the piston deflection and  $v$  is a voltage input that controls the current that generates the magnetic field;  $\delta$ ,  $\beta$ ,  $\kappa$  and  $n$  are parameters that are chosen so to adjust the hysteretic dynamics of the damper;  $c_0(v) = c_{0a} + c_{0b}v$  represents the voltage-dependent damping,  $k_0(v) = k_{0a} + k_{0b}v$  represents the voltage-dependent stiffness and  $\alpha(v) = \alpha_a + \alpha_b v$  is a voltage-dependent scaling factor.

Now we provide the numerical values of the model that we used in this study. This is because these numbers are required for the QFT controller development. Thus:  $\alpha_a = 332.7$  N/m,  $\alpha_b = 1862.5$  N·V/m,  $c_{0a} = 7544.1$  N·s/m,  $c_{0b} = 7127.3$  N·s·V/m,  $k_{0a} = 11375.7$  N/m,  $k_{0b} = 14435.0$  N·V/m,  $\delta = 4209.8$  m<sup>-2</sup>,  $\kappa = 10246$

and  $n = 2$ . This is a scaled version of the MR damper found in [31]. The parameter values of the suspension system are [28]:  $m_s=11739$  kg,  $m_u=300$  kg,  $k_s=252000$  N/m,  $c_s=10000$  N·s/m and  $k_t=300000$  N/m.

### 3 BACKSTEPPING CONTROLLER FORMULATION

The objective is to design an adaptive backstepping controller to regulate the suspension deflection with the aid of an MR damper thus providing safety and comfort while on the road. The adaptive backstepping controller will be designed in such a way that, for a given  $\gamma > 0$ , the state-dependent error variables  $e_1$  and  $e_2$  (to be defined later) accomplish the following  $H_\infty$  performance  $J_\infty < 0$ :

$$J_\infty = \int_0^\infty (\mathbf{e}^T \mathbf{R} \mathbf{e} - \gamma^2 \mathbf{w}^T \mathbf{w}) dt \quad (10)$$

where  $\mathbf{e} = (e_1, e_2)^T$  is a vector of controlled signals,  $\mathbf{R} = \text{diag}\{r_1, r_2\}$  is a positive definite matrix and  $\mathbf{w}$  is the vector of incoming disturbances.

Assume that  $a_k$  and  $a_c$  (in Equation (7)) are uncertain constant parameters whose estimated values are  $\hat{a}_k$  and  $\hat{a}_c$ , respectively. Thus, the errors between the estimates and the actual values are given by:

$$\tilde{a}_k = a_k - \hat{a}_k \quad (11)$$

$$\tilde{a}_c = a_c - \hat{a}_c \quad (12)$$

Let  $a_d = k_t[m_u(\rho + 1)]^{-1}$ ,  $a_n = \rho k_t[m_u(\rho + 1)^2]^{-1}$  and  $a_m = k_t m_u^{-1}$ . From Equations (5) - (6), it can be shown that the transfer functions from  $d(t)$  and  $f_{mr}(t)$  to  $z_1(t)$  are:

$$\frac{Z_1(s)}{D(s)} = \frac{-s(s^2 + a_c s + a_k)}{s^4 + a_c s^3 + (a_d + a_k)s^2 + a_d a_c s + a_d a_k - a_m a_n} \quad (13)$$

$$\frac{Z_1(s)}{F_{mr}(s)} = \frac{a_n a_f}{s^4 + a_c s^3 + (a_d + a_k)s^2 + a_d a_c s + a_d a_k - a_m a_n} \quad (14)$$

If the poles of the transfer functions of Equations (13) and (14) are in the left side of the  $s$  plane, then we can guarantee the bounded input - bounded output (BIBO) stability of  $Z_1(s)$  for any bounded input  $D(s)$  and  $F_{mr}(s)$ . Thus, the disturbance input  $d_i(t)$  in Equation (7) is also bounded. This boundedness condition will be used later in the controller formulation.

Finally, since  $d_i(t)$  is the only disturbance input to the suspension subsystem, the vector  $\mathbf{w}$  of the  $H_\infty$  performance objective as given in Equation (10) becomes:

$$J_\infty = \int_0^\infty (\mathbf{e}^T \mathbf{R} \mathbf{e} - \gamma^2 d_i^2) dt \quad (15)$$

In order to begin with the adaptive backstepping design, we firstly define the following error variable and its derivative:

$$e_1 = z_3 \quad (16)$$

$$\dot{e}_1 = \dot{z}_3 = z_4 \quad (17)$$

Now, the following Lyapunov function candidate is chosen:

$$V_1 = \frac{1}{2} e_1^2 \quad (18)$$

whose first-order derivative is:

$$\dot{V}_1 = e_1 \dot{e}_1 = e_1 z_4 \quad (19)$$

Equation (17) can be stabilized with the following virtual control input:

$$z_{4d} = -r_1 e_1 \quad (20)$$

$$\dot{z}_{4d} = -r_1 \dot{e}_1 = -r_1 z_4 \quad (21)$$

where  $r_1 > 0$ . Now define a second error variable and its derivative:

$$e_2 = z_4 - z_{4d} \quad (22)$$

$$\dot{e}_2 = \dot{z}_4 - \dot{z}_{4d} \quad (23)$$

Therefore,

$$\dot{V}_1 = e_2 z_4 = e_1 (e_2 - r_1 e_1) = e_1 e_2 - r_1 e_1^2 \quad (24)$$

On the other hand, the derivatives of the errors of the uncertain parameter estimations are given by:

$$\dot{\tilde{a}}_k = -\dot{\hat{a}}_k \quad (25)$$

$$\dot{\tilde{a}}_c = -\dot{\hat{a}}_c \quad (26)$$

Now, an augmented Lyapunov function candidate is chosen:

$$V = V_1 + \frac{1}{2} e_2^2 + \frac{1}{2r_k} \tilde{a}_k^2 + \frac{1}{2r_c} \tilde{a}_c^2 \quad (27)$$

Thus, by using Equations (22) - (26) and the fact that  $a_k = \tilde{a}_k + \hat{a}_k$  and  $a_c = \tilde{a}_c + \hat{a}_c$ , the derivative of  $V$  yields:

$$\begin{aligned} \dot{V} &= e_1 \dot{e}_1 + e_2 \dot{e}_2 + r_k^{-1} \tilde{a}_k \dot{\tilde{a}}_k + r_c^{-1} \tilde{a}_c \dot{\tilde{a}}_c \\ &= e_1 e_2 - r_1 e_1^2 + e_2 \dot{d}_i - a_k z_3 e_2 - a_c z_4 e_2 + a_f f_{mr} e_2 - \\ &\quad r_1 z_4 e_2 - r_k^{-1} \tilde{a}_k \dot{\hat{a}}_k - r_c^{-1} \tilde{a}_c \dot{\hat{a}}_c \\ &= e_1 e_2 - r_1 e_1^2 + e_2 \dot{d}_i + a_f f_{mr} e_2 - r_1 z_4 e_2 - r_k^{-1} \tilde{a}_k \dot{\hat{a}}_k - \\ &\quad (\tilde{a}_k + \hat{a}_k) z_3 e_2 - (\tilde{a}_c + \hat{a}_c) z_4 e_2 - r_c^{-1} \tilde{a}_c \dot{\hat{a}}_c \\ &= e_1 e_2 - r_1 e_1^2 + e_2 \dot{d}_i - \tilde{a}_k (z_3 e_3 + r_k^{-1} \dot{\hat{a}}_k) - \hat{a}_k z_3 e_2 - \\ &\quad \tilde{a}_c (z_4 e_2 + r_c^{-1} \dot{\hat{a}}_c) - \hat{a}_c z_4 e_2 + a_f f_{mr} e_2 - r_1 z_4 e_2 \end{aligned} \quad (28)$$

Now consider the following adaptation laws:

$$z_3 e_1 + r_k^{-1} \dot{\hat{a}}_k = 0 \quad (29)$$

$$z_4 e_2 + r_c^{-1} \dot{\hat{a}}_c = 0 \quad (30)$$

Substitution of Equations (29) and (30) into Equation (28) yields:

$$\dot{V} = -r_1 e_1^2 + e_2 \dot{d}_i + e_2 (e_1 - \hat{a}_k z_3 - \hat{a}_c z_4 + a_f f_{mr} - r_1 z_4) \quad (31)$$

By choosing the following control law:

$$f_{mr} = -\frac{e_1 - \hat{a}_k z_3 - \hat{a}_c z_4 - r_1 z_4 + r_2 e_2 + e_2 (2\gamma)^{-2}}{a_f} \quad (32)$$

with  $\gamma > 0$  and  $r_2 > 0$ , we get:

$$\begin{aligned}\dot{V} &= -r_1 e_1^2 + e_2 d_i - r_2 e_2^2 - e_2^2 (2\gamma)^{-2} \\ &= -r_1 e_1^2 + e_2 d_i - r_2 e_2^2 - e_2^2 (2\gamma)^{-2} + \gamma^2 d_i^2 - \gamma^2 d_i^2 \\ &= -r_1 e_1^2 - r_2 e_2^2 + \gamma^2 d_i^2 - (\gamma d_i - e_2 (2\gamma)^{-2})^2 \\ \dot{V} &\leq -r_1 e_1^2 - r_2 e_2^2 + \gamma^2 d_i^2\end{aligned}\quad (33)$$

The objective of guaranteeing global boundedness of trajectories is equivalently expressed as rendering  $\dot{V}$  negative outside a compact region. As stated earlier, the disturbance input  $d_i$  is bounded as long as the poles of the transfer functions (13) and (14) are in the left side of the  $s$  plane. When this is the case, the boundedness of the input disturbance  $d_i$  guarantees the existence of a small compact region  $D \subset \mathbb{R}^2$  (depending on  $\gamma$  and  $d_i$  itself) such that  $\dot{V}$  is negative outside this set. More precisely, when  $r_1 e_1^2 + r_2 e_2^2 < \gamma^2 d_i^2$ ,  $\dot{V}$  is positive and then the error variables are increasing values. Finally, when the expression  $r_1 e_1^2 + r_2 e_2^2$  is greater than  $\gamma^2 d_i^2$ ,  $\dot{V}$  is then negative. This implies that all the closed-loop trajectories have to remain bounded, as we wanted to show. Now, under zero initial conditions, we can write:

$$\begin{aligned}\int_0^\infty \dot{V} dt &\leq -\int_0^\infty r_1 e_1^2 dt - \int_0^\infty r_2 e_2^2 dt + \int_0^\infty \gamma^2 d_i^2 dt \\ V|_{t=\infty} - V|_{t=0} &\leq -\int_0^\infty \mathbf{e}^T \mathbf{R} \mathbf{e} dt + \gamma^2 \int_0^\infty d_i^2 dt \\ J_\infty &= \int_0^\infty (\mathbf{e}^T \mathbf{R} \mathbf{e} - \gamma^2 d_i^2) dt \leq -V|_{t=\infty} \leq 0\end{aligned}\quad (34)$$

Thus, the adaptive backstepping controller satisfies the  $H_\infty$  performance and the asymptotic stability of the system is guaranteed.

The control force given by Equation (32) can be used to drive an actively controlled damper. However, the fact that semiactive devices cannot inject energy into a system, makes necessary the modification of this control law in order to implement it with a semiactive damper; that is, semiactive dampers cannot apply force to the system, only absorb it. There are different ways to perform this [26], [32]. In this work, we will calculate the MR damper voltage making use of its mathematical model. Thus, the following control law is proposed:

$$v = \frac{-e_1 - \hat{a}_z z_3 + \hat{a}_c z_4 + r_1 z_4 - r_2 e_2}{a_f (c_{0b} z_4 + k_{0b} z_3 + \alpha_b \zeta)} + \frac{-e_2 (2\gamma)^{-2} + a_f (c_{0a} z_4 + k_{0a} z_3 + \alpha_a \zeta)}{a_f (c_{0b} z_4 + k_{0b} z_3 + \alpha_b \zeta)}\quad (35)$$

provided that  $a_f (c_{0b} z_4 + k_{0b} z_3 + \alpha_b \zeta) \neq 0$ ; otherwise,  $v = 0$ .

The same process followed to obtain the control law of Equation (32) can be used to demonstrate that the control law of Equation (35) does stabilize the system. Begin by replacing Equation (8) into Equation (31) in order to obtain:

$$\begin{aligned}\dot{V} &= -r_1 e_1^2 + e_2 d_i + e_2 [e_1 - \hat{a}_k z_3 - \hat{a}_c z_4 + \\ & a_f (c_{0a} z_4 + k_{0a} z_3 + \alpha_a \zeta) + \\ & a_f (c_{0b} z_4 + k_{0b} z_3 + \alpha_b \zeta) v - r_1 z_4]\end{aligned}\quad (36)$$

Thus, by replacing the control law of Equation (35) into Equation (36) we also get  $\dot{V} \leq -r_1 e_1^2 - r_2 e_2^2 + \gamma^2 d_i^2$  and, as previously stated, the stability of the system is guaranteed.

## 4 QUANTITATIVE FEEDBACK THEORY

QFT is a frequency control methodology based on the notion that feedback is necessary only when there is uncertainty and non-measurable disturbances actuating on the plant. The basic developments with QFT are focused on the control design problem for uncertain linear time invariant (LTI) systems like the one shown in Figure 2. In this figure,  $\mathbf{R}$  represents the command input set,  $\mathbf{P}$  is the plant set and  $\mathbf{T}$  is the closed loop transfer function set. For each  $R(s) \in \mathbf{R}$  and  $P(s) \in \mathbf{P}$ , the output will be  $Y(s) = T(s)R(s)$  for some  $T(s) \in \mathbf{T}$ . For a large class of problems, a pair of controllers  $F(s)$  and  $G(s)$  can be found to guarantee  $Y(s) = T(s)R(s)$ .

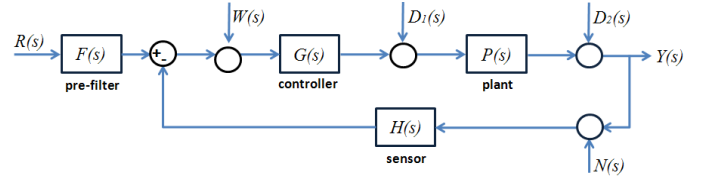


Fig. 2. Schematic of the QFT control system.

The uncertain plant model  $P(s)$  and its frequency and time domain specifications are represented in the Nichols chart through the use of Horowitz-Sidi bounds. These bounds determine the regions where the nominal loop transfer function  $L_0(s) = G(s)P_0(s)H(s)$  may lie so that all the design specifications can be achieved [33]. The controller development is explained in what follows.

In order to begin with the QFT controller formulation, first recall the suspension subsystem as given in Equation (7). The Laplace transform from the damper force  $f_{mr}$  to the deflection  $z_3(t)$  is given by:

$$\begin{aligned}Z_3(s) &= \frac{m_u \left(\frac{m_s}{m_u} + 1\right)^2}{\Delta_a(s)} F_{mr}(s) + \frac{m_s \left(\frac{m_s}{m_u} + 1\right) k_t}{\Delta_a(s)} D_i(s) \\ \Delta_a(s) &= (m_u m_s + m_s^2) s^2 + \left(m_u c_s + \frac{m_s^2 c_s}{m_u} + 2m_s m_u\right) s + \\ & \frac{m_s^2}{m_u} (k_t + k_s) + 2k_s (m_s + m_u)\end{aligned}\quad (37)$$

where  $D_i(s) = k_t/m_u Z_i(s)$  is the input disturbance. Since the MR damper is a nonlinear device, an approximation to an uncertain linear plant is proposed to solve this problem. Consider the MR damper model of Equation

(8). It can be decomposed into two parts: one linear and the other nonlinear. Thus:

$$f_{lin} = (c_{0a} + c_{0b}v)z_4 + (k_{0a} + k_{0b}v)z_3 = a_1z_4 + a_2z_3 \quad (39)$$

$$f_{nonlin} = (\alpha_a + \alpha_bv)\zeta_0 = \alpha_b\zeta_0v_d \quad (40)$$

$$f_{mr} = f_{lin} + f_{nonlin} \quad (41)$$

$$v_d = \frac{\alpha_a}{\alpha_b} + v \quad (42)$$

From Equations (39) - (42), it is observed that the parameters  $a_1$  and  $a_2$  vary only with the input voltage. The third parameter,  $\zeta_0$  is a bounded parameter. See Figure 3: at high velocities,  $\zeta$  is approximately constant and thus,  $\zeta_0$  could take either the maximum or the minimum value depending on the signs of the velocity. In this way, Equation (8) can be seen as a linear system with three uncertain parameters, namely,  $a_1$ ,  $a_2$  and  $\zeta_0$  which describes the dynamics of the damper. The damper dynamics now appear to follow the Bingham model. Figure 4 illustrates this approach with a sinusoidal displacement excitation at three different levels of voltage.

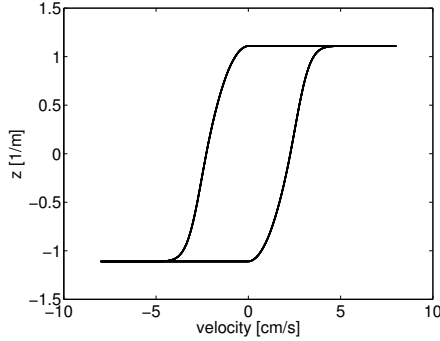


Fig. 3. Example of a hysteresis loop.

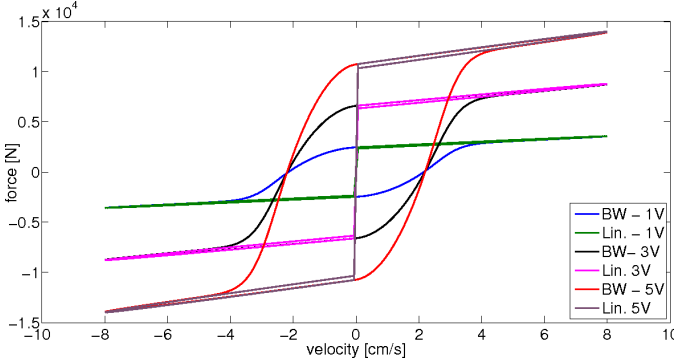


Fig. 4. Description of the MR damper as an uncertain plant.

The Laplace transform of Equation (41) is:

$$F_{mr}(s) = a_1sZ_4(s) + a_2Z_3(s) + \alpha_b\zeta_0V_d(s) \quad (43)$$

Substitution of Equation (43) into Equation (37) yields:

$$Z_3(s) = \frac{m_u \left( \frac{m_s}{m_u} + 1 \right)^2 \alpha_a \zeta_0}{\Delta_{sa}(s)} V_d(s) + \frac{m_s \left( \frac{m_s}{m_u} + 1 \right) k_t}{\Delta_{sa}(s)} D_i(s) = P(s)V_d(s) + D_i^*(s) \quad (44)$$

$$\Delta_{sa}(s) = (m_s^2 + m_u m_s) s^2 + \left( \frac{m_s^2}{m_u} + 2m_s + m_u \right) (c_s + a_1) s + \frac{m_s^2}{m_u} (k_t + k_s + a_2) + (2m_s + m_u) (k_s + a_2) \quad (45)$$

Thus, the controller can then be designed for the uncertain plant  $P(s)$  with unknown input disturbance  $D_i^*(s)$  and the input voltage can be obtained from  $v = -(v_d + \alpha_a/\alpha_b)$ . In this case, we assume that the sprung mass and the tyre stiffness are the parameters that vary the most with respect to the others. Thus, the uncertain parameters of the plant are:  $a_1 \in [754.41, 4318.06]$  N·s/m,  $a_2 \in [1137, 6855.07]$  N/m,  $\zeta_0 \in \{-1.11, 1.11\}$  m<sup>-1</sup> (only one of two values),  $k_t \in [240000, 360000]$  N/m and  $m_s \in [9391, 14087]$  kg. The other parameters are those given in Section 2. The controller design parameters are: robust performance  $W_{s1} = 2$ , disturbance rejection  $W_{s3} = 0.03$  and control effort  $W_{s4} = 150$ .

The next step in the controller design is to generate the templates. This is a representation in the Nichols chart of the plant model  $P(j\omega)$  at each frequency of interest and for each possible value of the uncertain parameters. Figure 5 shows the templates for this model for the frequencies 10, 30 and 60 rad/s. Now the design specifications are transformed into a set of restriction curves or bounds, known as Horowitz-Sidi bounds, for each frequency of interest in the Nichols chart. For each frequency and each design specification, there is one bound but only the most restrictive ones per frequency are kept. The bounds for this problem are shown in Figure 6. The dotted blue, red and green lines are the bounds. The dotted magenta line is the closed loop response  $L_0(s)$  with a proportional controller with gain  $K = 1$ . The objective now is to move the closed loop response line as close as possible to the bounds in such a way that at each frequency of interest, it lies below the bound. This is done by adding a gain, poles and zeros to the controller. The black solid line is the result of doing this. The resulting controller is:

$$G_1(s) = \frac{61.34(5.4 \times 10^{-3}s + 1)(6.84 \times 10^{-2}s + 1)}{(2.83 \times 10^{-3}s^2 + 5.72 \times 10^{-2}s + 1)} \times \frac{(1.49 \times 10^{-4}s^2 + 1.04 \times 10^{-2}s + 1)}{(2.60 \times 10^{-4}s^2 + 7.77 \times 10^{-3}s + 1)} \quad (46)$$

Figure 6 shows that the closed-loop response lies right next to the bounds at the frequencies of interest and does not cross the ray  $(0, 180^\circ)$ . Thus, according to QFT, the closed loop system using this controller is stable in

the presence of uncertainties. Finally, Figure 7 shows the performance of the controller regarding the design specifications (robustness, disturbance rejection and control effort). In all cases, the closed loop response lies below the limits imposed and thus, the design requirements are achieved.

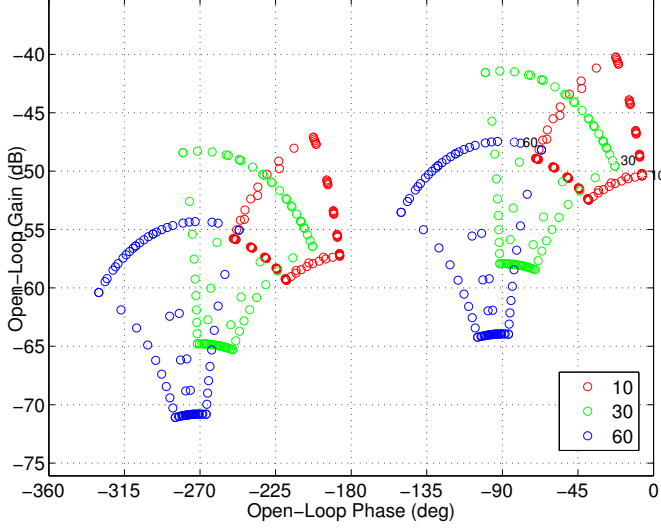


Fig. 5. Templates of the suspension system with MR damper.

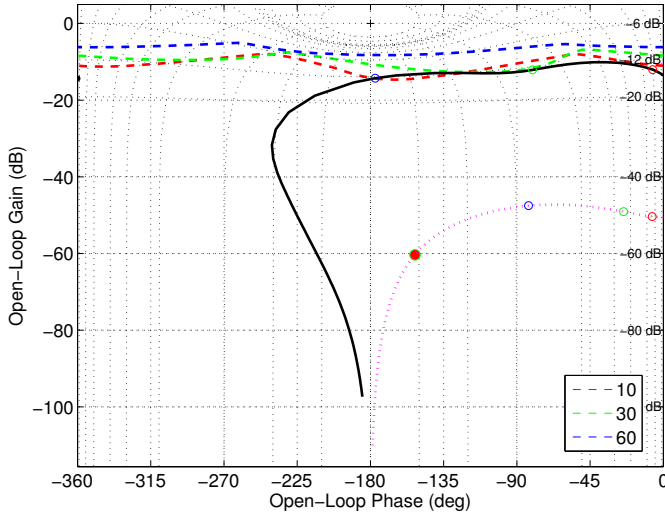


Fig. 6. Initial loop (before shaping) and final loop (after shaping).

## 5 NUMERICAL RESULTS

The controllers of Equations (35) and (46) were implemented in MATLAB/Simulink in order to evaluate their performance. Each simulation was run during 10 seconds. The performance indices shown in Table 1 were used to numerically compare the controller performance with the case when there is no controller. Indices

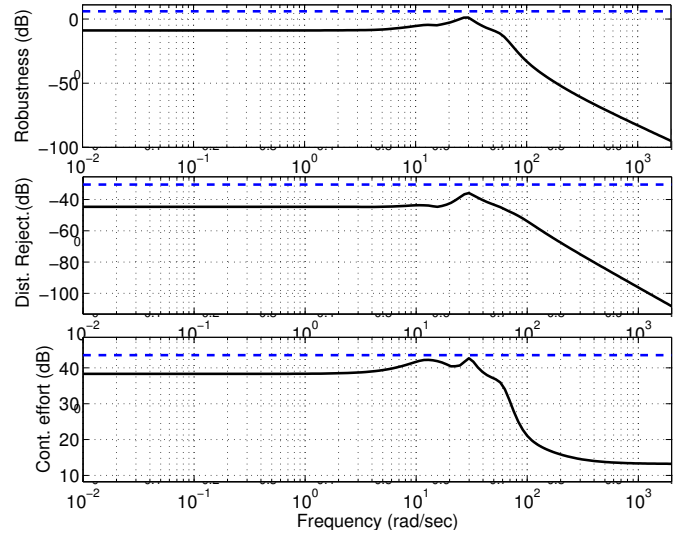


Fig. 7. Performance analysis of the controller of Equation 46 (robustness, disturbance rejection and control effort).

$J_1 - J_3$  show the ratio between the peak response of the controlled suspension system (displacement, velocity and acceleration) and that of the uncontrolled system. Indices  $J_4 - J_6$  are the normalized ITSE (integral of the time squared error) signals that indicate how much the displacement, velocity and acceleration are attenuated compared to the uncontrolled case. Index  $J_7$  is the relative maximum control effort with respect to the weight of the suspension system. Small indices indicate good control performance.

Index	Definition
$J_1 = \frac{\max x_3(t) _{cont}}{\max x_3(t) _{unc}}$	Norm. peak suspension deflection.
$J_2 = \frac{\max \dot{x}_4(t) _{cont}}{\max \dot{x}_4(t) _{unc}}$	Norm. peak sprung mass velocity.
$J_3 = \frac{\max \ddot{x}_4(t) _{cont}}{\max \ddot{x}_4(t) _{unc}}$	Norm. peak sprung mass acceleration.
$J_4 = \frac{\int_0^T t x_{3cont}^2(t) dt}{\int_0^T t x_{3unc}^2(t) dt}$	Norm. suspension deflection ITSE.
$J_5 = \frac{\int_0^T t \dot{x}_{4cont}^2(t) dt}{\int_0^T t \dot{x}_{4unc}^2(t) dt}$	Norm. sprung mass velocity ITSE.
$J_6 = \frac{\int_0^T t \ddot{x}_{4cont}^2(t) dt}{\int_0^T t \ddot{x}_{4unc}^2(t) dt}$	Norm. sprung mass acceleration ITSE.
$J_7 = \frac{\max f_{mr}(t) }{w_s}$	Maximum control effort.

TABLE 1  
Performance indices.

As a matter of comparison, the performances of the controllers discussed in this paper will be contrasted to another designed by the authors in a previous work [26]. The controller is a modification of the clipped optimal controller approach by Dyke et al. [34]. The commanding voltage to the MR damper is computed according to:

$$v = V_{max} H(f_{mr} - f_{meas}) f_{meas} \quad (47)$$

where  $V_{max}$  is the maximum allowed voltage (5 V in this case),  $H \cdot$  is the Heaviside function,  $f_{meas}$  is the actual MR damper force as measured by a sensor and  $f_{mr}$  is the control forced computed by the following QFT controller:

$$G_2(s) = \frac{176168(3.78 \times 10^{-2}s^2 + 1.86 \times 10^{-1}s + 1)}{6.91 \times 10^{-2}s^2 + 1.38 \times 10^{-1}s + 1} \times \frac{3.07 \times 10^{-4}s^2 + 1.76 \times 10^{-2}s + 1}{6.27 \times 10^{-4}s^2 + 1.87 \times 10^{-2}s + 1} \quad (48)$$

Before proceeding with the controller performance, we will examine the dynamics of the suspension system when subject to a bump on the road and to a random input. The behavior of the system is analyzed in the case when the voltage is set to 0 V, that is, no current is flowing through the MR damper coils. The results are shown in Figures 8 and 9, the suspension system dynamics is practically the same as if there were no damper installed. The effect of such low damping is minimum and in consequence, it does not destabilize the system.

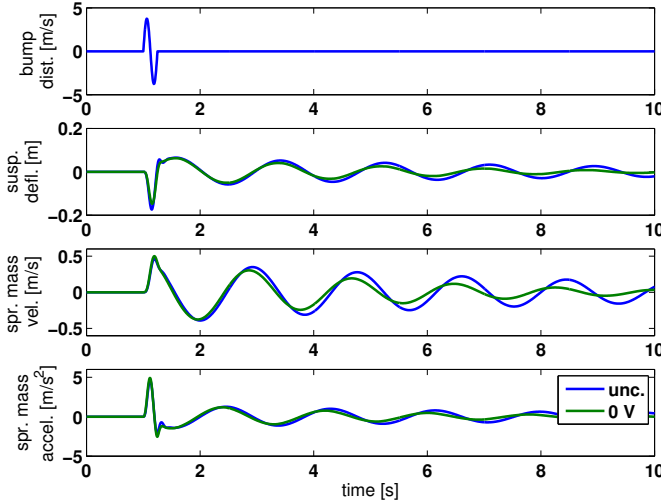


Fig. 8. Suspension subsystem when the damper is in the 'off' mode subject to a bump input.

In order to analyze the controllers, we begin by simulating the response when the suspension system is subject to a bump on the road. Figure 10 depicts the tyre deflection and the unsprung mass velocity. The suspension deflection, the sprung mass velocity and acceleration are depicted in Figure 11. A comparison of both controllers with respect to the uncontrolled case is presented there. First of all, it is worth noting that the tyre deflection and the unsprung mass velocity are reduced with both controllers despite these variables were not directly included in the controller formulation. The suspension deflection peak is reduced with both controllers and this signal is attenuated along the time. The effect of the backstepping controller is notorious

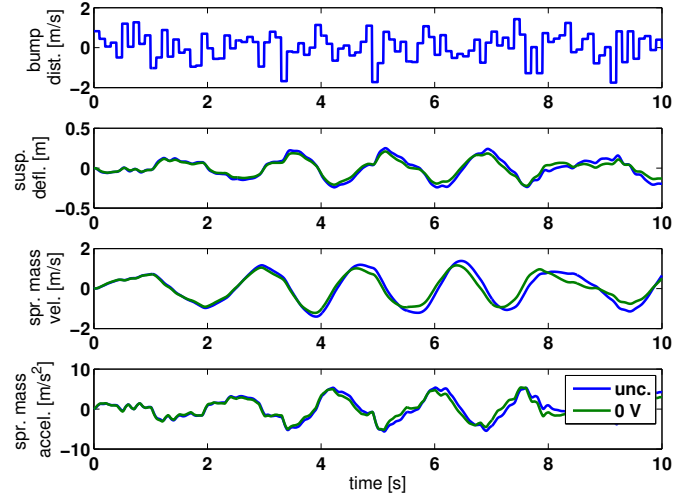


Fig. 9. Suspension subsystem when the damper is in the 'off' mode subject to a random input.

here due to the suspension deflection reduction. The sprung mass velocity peak is not reduced with any controller; instead it remains almost the same as in the uncontrolled case. However, the attenuation of the velocity is achieved along the time as it can be observed. The same thing happens with the acceleration. In this case, however, there is an increase in the peak acceleration although it is thereafter attenuated by both controllers. Figure 12 shows the control effort of the damper using both controllers as well as the control signals.

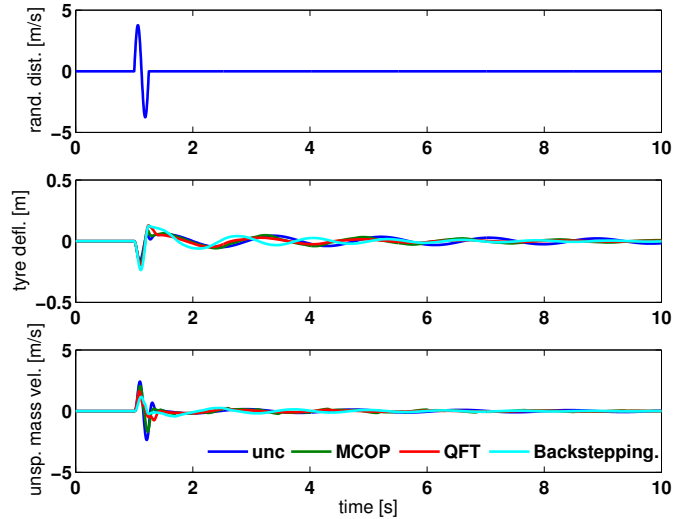


Fig. 10. Disturbance input and tyre subsystem system response when subject to a bump on the road.

The values of the performance indices for this case are shown in Table 2. The indices confirm some of the visual observations. In fact, both controllers reduce the peak deflection but the peak velocity and peak acceleration are increased. However, both controllers are able to reduce the three signals along the time if we compare them



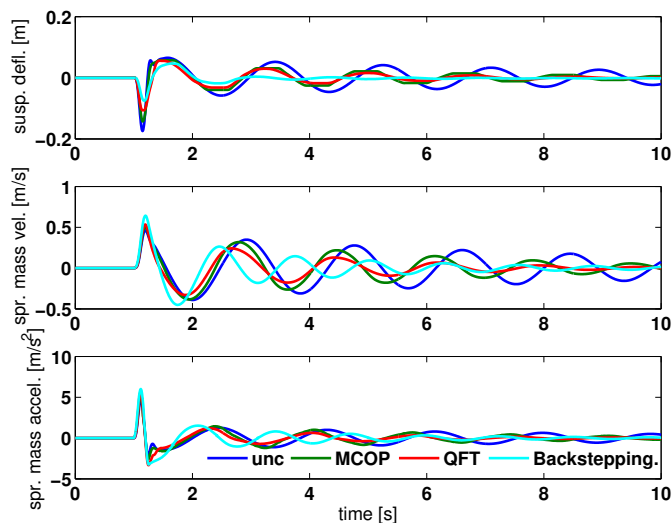


Fig. 11. Suspension subsystem response when subject to a bump on the road (suspension deflection, sprung mass velocity and sprung mass acceleration).

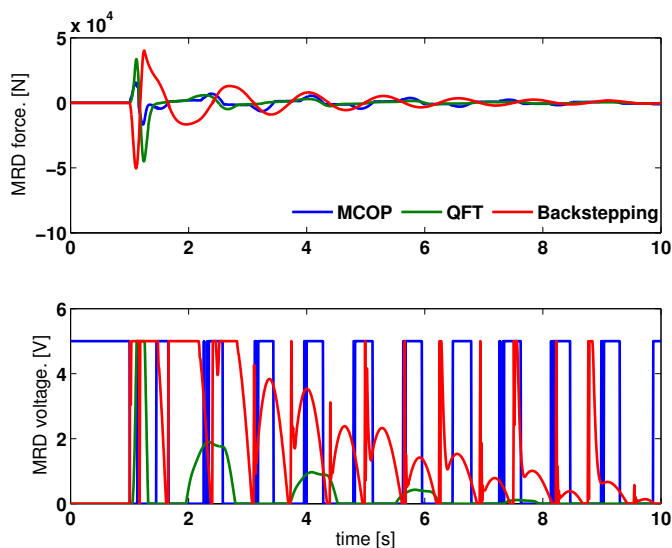


Fig. 12. MR damper response when subject to a bump on the road.

with the uncontrolled case. The greater peak velocity and acceleration achieved with the backstepping controller may be caused by the greater control effort as can be seen in index  $J_7$ . In this case, the backstepping controller performs better than the QFT controller. In comparison to these controllers, the QFT-modified clipped optimal controller shows a high peak in the suspension deflection caused by the low damping required to keep the system under acceptable limits. Furthermore, since the QFT-modified controller switches between two control levels, the transition between these states makes the system to respond in a less smooth way than that expected with the other controllers that continuously change the control level by taking every possible value in the voltage range.

Index	Backstepping	QFT	MCOP
$J_1$	0.4287	0.6112	0.8207
$J_2$	1.3864	1.1567	1.0935
$J_3$	1.2965	1.2052	1.0772
$J_4$	0.0715	0.2094	0.3733
$J_5$	0.2777	0.2495	0.5529
$J_6$	0.6742	0.4350	0.7176
$J_7$	0.4395	0.3915	0.1453

TABLE 2

Performance indices of the road bump disturbance case.

In a second simulation, the system was subject to a random input. This input is shown in Figure 13 as well as the tyre deflection and the unsprung mass velocity. The suspension deflection, sprung mass velocity and acceleration are shown in Figure 14. The MR damper response is shown in Figure 15. As in the previous case, the tyre deflection and the unsprung mass velocity are kept within the limits of the uncontrolled case although there is no apparent reduction in these signals. With respect to the suspension deflection it is possible to observe a reduction when compared to the uncontrolled case. Table 3 provides us with a better insight in this case. As depicted in Figure 14, there is a considerable reduction in the suspension deflection as well as a low reduction in the sprung mass velocity. However, according to the indices, both controllers increase the peak sprung mass acceleration. In this case, the QFT controller performs better reducing both velocity and acceleration and with less control effort than the backstepping controller. As in the previous case, the QFT-modified clipped optimal controller does not perform as good as any of the other controllers.

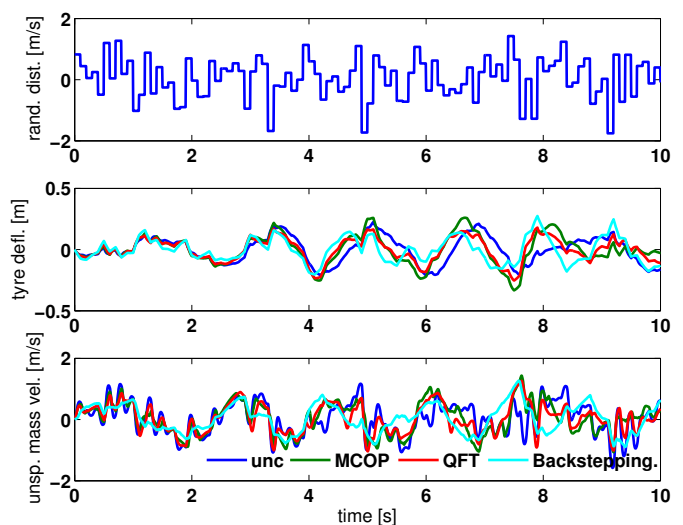


Fig. 13. Disturbance input and tyre subsystem response when subject to a random unevenness on the road.

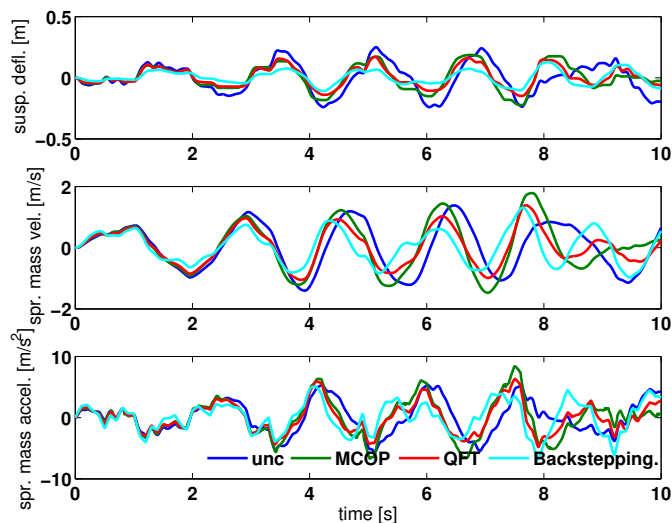


Fig. 14. Suspension subsystem response when subject to a random unevenness on the road (suspension deflection, sprung mass velocity and sprung mass acceleration).

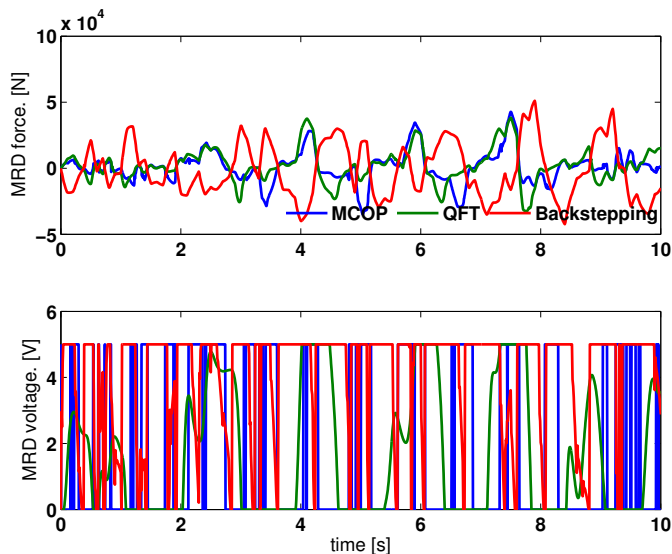


Fig. 15. MR damper response when subject to a random unevenness on the road.

## 6 CONCLUSIONS

In this paper we have proposed two different semiactive controllers for a suspension system that makes use of a magnetorheological damper. This class of damper is known due to its nonlinear dynamics that makes mandatory the use of nonlinear control techniques for an appropriate performance. We have gone one step beyond with respect to previous works at designing two semiactive controllers that make use of the full range of the voltage control signal and considering the nonlinearities involved in the MR damper dynamics.

Index	Backstepping	QFT	MCOP
$J_1$	0.5118	0.6848	0.8950
$J_2$	0.9337	0.9893	1.2722
$J_3$	1.2146	1.1264	1.4936
$J_4$	0.2191	0.4080	0.6876
$J_5$	0.5359	0.5645	0.8000
$J_6$	0.8905	0.7581	1.2368
$J_7$	0.4441	0.3325	0.3717

TABLE 3  
Performance indices of the random unevennes disturbance case.

The first semiactive controller was designed following the adaptive backstepping technique with some  $H_\infty$  constraints. This technique allowed us for including the nonlinearities and uncertainties of the system in a single nonlinear control law. The second controller was designed with QFT methodology. Since QFT requires a linear time invariant system model for its development, we proposed a representation of the MR damper dynamics as a linear plant with uncertain parameters that approximated its dynamics. Both controllers were simulated in MATLAB/Simulink. Both controllers showed a satisfactory performance since important variables such as deflection were reduced and/or kept within acceptable limits. Despite the controllers performed differently in the scenarios studied, they both accomplished the objective of reducing the response of the suspension system.

In futures works it is worth exploring the possibility of implementing switching systems in order to model the nonlinear dynamics of the MR damper and thus, improve the performance of the control systems. Some recent works could provide us with the tools for implementing such a system (see for instance [25] and [35]). Furthermore, it is worth exploring the effect of time delays in measurements and communication channels. Time delays are inherent to most modern control systems and, if not handles appropriately, may become problematic in the system. Electronic suspension control systems implemented in vehicles such as cars, trains, trucks and airplanes, share the resources in a large system with a high number of tasks and thus, it is mandatory to account for the delays inherent to it. Discretization and inclusion of time-delay constraints are to be added to the controllers proposed in this work in order to keep the good performance when implemented in control networks.

## REFERENCES

- [1] L. Zhu, C.R. Knospe, "Modeling of nonlaminated electromagnetic suspension systems", IEEE/ASME Transactions on Mechatronics, Vol. 15, no. 1, pp. 59-69, 2010.

- [2] H. Wang, J.T. Xing, W.G. Price, W. Li, "An investigation of an active landing gear system to reduce aircraft vibrations caused by landing impacts and runway excitations", *Journal of Sound and Vibration*, Vol. 317, pp. 50-66, 2008.
- [3] D.S. Wu, H.B. Gu, H. Liu, "GA-based model predictive control of semi-active landing gear", *Chinese Journal of Automatics*, Vol. 20, pp. 47-54, 2007.
- [4] J.D. Carlson: Magnetorheological Fluid Actuators, in: *Adaptronics and Smart Structures. Basics, Materials, Design and Applications*, edited by H. Janocha. Springer, 1999.
- [5] G.L. Ghiringhelli, S. Gualdi, "Evaluation of a landing gear semi-active control system for complete aircraft landing", *Aerotecnica Missili e Spazio*, Vol. 83, 21-31, 2004.
- [6] G. Pouly, T.H. Huynh, J.P. Lauffenburger, M. Basset, "Active shimmy damping using Fuzzy Adaptive output feedback control", *10<sup>th</sup> International Conference on Control, Automation, Robotics and Vision*, Hanoi, Vietnam, 2008.
- [7] G.Z. Yao, F.F. Yap, G. Chen, W.H. Li, S.H. Yeo, "MR damper and its application for semi-active control of vehicle suspension system", *Mechatronics*, Vol. 12(7), pp. 963-973, 2002.
- [8] V. Sankaranarayanan, M.E. Emekli, B. A. Güvenç, L. Güvenç, E.S. Öztürk, Ş.S. Ersolmaz, I.E. Eyol, M. Sinal, "Semiactive suspension control of a light commercial vehicle", *IEEE/ASME Transactions on Mechatronics*, Vol. 13, no. 5, pp. 598-604, 2008.
- [9] D.L. Guo, H.Y. Hu, J.Q. Yi, "Neural network control for a semi-active vehicle suspension with a magnetorheological damper", *Journal of Vibration and Control*, Vol. 10, pp. 461-471, 2004.
- [10] N. Karlsson, M. Dahleh, D. Hrovat, "Nonlinear active suspension with preview", *Proceedings of the American Control Conference*, Arlington, Virginia, USA, June 25-27, 2001.
- [11] H. Du, J. Lam and K.Y. Sze, "Non-fragile output feedback  $H_\infty$  vehicle suspension control using genetic algorithm", *Engineering Applications of Artificial Intelligence*, Vol. 16, pp. 667-680, 2003.
- [12] H. Du, K.Y. Sze and J. Lam, "Semi-active  $H_\infty$  control of vehicle suspension with magneto-rheological dampers", *Journal of Sound and Vibration*, Vol. 283 (3-5), pp. 981-996, 2005.
- [13] H. Gao, J. Lam and C. Wang, "Multi-objective control of vehicle active suspension systems via load-dependent controllers", *Journal of Sound and Vibration*, Vol. 290 (3-5), pp. 654-675, 2005.
- [14] H. Gao, W. Sun and P. Shi, "Robust sampled-data  $H_\infty$  control for vehicle active suspension systems", *IEEE Transactions on Control Systems Technology*, Vol. 18 (1), pp.238-245, 2010.
- [15] H. Gao, Y. Zhao and W. Sun, "Input-delayed control of uncertain seat suspension systems with human-body model", *IEEE Transactions on Control Systems Technology*, Vol. 18(3), pp. 591-601, 2010.
- [16] S.-L. Chen, C.-C. Weng, "Robust control of a voltage-controlled three-pole active magnetic bearing system", *IEEE/ASME Transactions on Mechatronics*, Vol. 15, no. 3, pp. 381-388, 2010.
- [17] T. Wang, S. Tong, Y. Li, "Robust adaptive fuzzy control for nonlinear system with dynamic uncertainties based on backstepping", *International Journal of Innovative Computing, Information and Control*, Vol. 5, no. 9, pp. 2675-2688, 2009.
- [18] S. Tong, Y. Li, T. Wang, "Adaptive fuzzy backstepping fault-tolerant control for uncertain nonlinear systems based on dynamic surface", *International Journal of Innovative Computing, Information and Control*, Vol. 5, no. 10(A), pp. 3249-3261, 2009.
- [19] M. Zapateiro, N. Luo, H.R. Karimi, J. Vehí, "Vibration control of a class of semiactive suspension system using neural network and backstepping techniques", *Mechanical Systems and Signal Processing*, Vol. 23, 1946-1953, 2009.
- [20] T.T. Nguyen, T.H. Bui, T.P. Tran, S.B. Kim, "A hybrid control of active suspension system using  $H_\infty$  and nonlinear adaptive controls", *IEEE International Symposium on Industrial Electronics*, Pusan, Korea, 2001.
- [21] A. Liberzon, D. Rubinstein, P.O. Gutman, "Active suspension for single wheel station of off-road track vehicle", *International Journal of Robust and Nonlinear Control*, Vol. 11, pp. 977-999, 2001.
- [22] A.M. Amani, A.K. Sedigh, M.J. Yazdanpanah, "A QFT approach to robust control of automobiles active suspension", *5<sup>th</sup> Asian Control Conference*, Melbourne, Australia, July 20-23, 2004.
- [23] E.Z. Taha, G.S. Happawana, Y. Hurmulzlu, "Quantitative Feedback Theory (QFT) for chattering reduction and improve tracking in sliding mode control", *Proceedings of the American Control Conference*, Arlington, Virginia, USA, June 25-27, 2001.
- [24] W. Li and X. Liu, "Robust adaptive tracking control of uncertain electrostatic micro-actuators with H-infinity performance", *Mechatronics*, vol. 19, pp. 591-597, 2009.
- [25] L. Zhang, P. Shi, E.K. Boukas, C. Wang, " $H_\infty$  model reduction for uncertain switched linear discrete-time systems", *Automatica*, Vol. 11, no. 11, pp. 2944-2949, 2008.
- [26] M. Zapateiro, H.R. Karimi, N. Luo, B.F. Spencer, Jr., "Real-time hybrid testing of semiactive control strategies for vibration reduction in a structure with MR damper", *Structural Control and Health Monitoring*, Vol. 17(4), pp.427-451, 2010.
- [27] M. Zapateiro, H.R. Karimi, N. Luo, B.F. Spencer Jr., "Frequency domain control based on Quantitative Feedback Theory for vibration suppression in structures equipped with magnetorheological dampers", *Smart Materials and Structures*, Vol. 18, doi: 10.1088/0964-1726/18/9/095041, 2009.
- [28] N. Karlsson, A. Teel, D. Hrovat, "A backstepping approach to control of active suspensions", *Proceedings of the 40th IEEE Conference on Decision and Control*, Orlando, Florida, USA, 2001.
- [29] M. Krstic, I. Kanellakopoulos, O. Kokotovic, "Nonlinear and Adaptive Control Design", John Wiley and Sons, Inc., 1995.
- [30] B.F. Spencer, Jr., S.J. Dyke, M. Sain, J.D. Carlson, "Phenomenological model of a magnetorheological damper", *ASCE Journal of Engineering Mechanics*, Vol. 123, pp. 230-238, 1997.
- [31] J. Carrion, B.F. Spencer, Jr., "Model-based strategies for real-time hybrid testing", *Technical Report, University of Illinois at Urbana-Champaign*, Available at: <http://hdl.handle.net/2142/3629>, 2007.
- [32] A. Bahar, F. Pozo, L. Acho, J. Rodellar, A. Barbat, "Hierarchical semi-active control of base-isolated structures using a new inverse model of magnetorheological dampers", *Computers and Structures*, Vol. 88, pp. 483-496, 2010.
- [33] C. Houpis, S. Rasmussen, M. García-Sanz, "Quantitative Feedback Theory: Fundamentals and Applications", CRC Press, Boca Raton, Florida, USA, 2005.
- [34] S.J. Dyke, B.F. Spencer Jr., M.K. Sain, J.D. Carlson, "Modeling and control of magnetorheological dampers for seismic response reduction", *Smart Materials and Structures*, Vol. 5, pp. 565-757, 1996.
- [35] L. Zhang, C. Wang, L. Chen, "Stability and stabilization of a class of multimode linear discrete-time systems with polytopic uncertainties", *IEEE Transactions of Industrial Electronics*, Vol. 56 (9), pp. 3684-3692.